THE ASTROPHYSICAL JOURNAL SUPPLEMENT SERIES, 132:403–409, 2001 February

OSCILLATOR STRENGTHS OF TRANSITIONS IN Ti II IN THE VISIBLE AND ULTRAVIOLET REGIONS

J. C. PICKERING, A. P. THORNE, AND R. PEREZ
Blackett Laboratory, Imperial College, London SW7 2BZ; and ISO Data Centre, Astrophysics Division, ESA, Villafranca, Spain
Received 2000 June 28; accepted 2000 September 21

ABSTRACT

The relative intensities of 694 emission lines of Ti II between 187 and 602 nm from 89 levels have been measured by high-resolution Fourier transform spectrometry, using a hollow cathode lamp as light source. The spectral response function of the instrument was determined with calibrated tungsten halogen and deuterium lamps. Errors due to self-absorption in strong lines were eliminated by running the lamp at different currents. At least 95% of the predicted transition intensity has been measured for 83 of these levels, allowing reliable branching fractions to be found. The branching fractions have been combined with 39 measured and 44 computed lifetimes to give absolute transition probabilities for 624 lines. These agree well with the most recent values for 55 of the lines obtained in a similar way from seven of the measured lifetimes.

Subject headings: atomic data — line: identification — stars: abundances — techniques: spectroscopic
On-line material: machine-readable tables

1. INTRODUCTION

Laboratory spectral data of much higher quality than hitherto are required to support current astrophysical observations, both ground- and space-based. The spectra of the iron group elements are particularly important because of their high abundance and line-rich spectra, and in B, A, and F stars the first stage of ionization is predominant, e.g., Johansson (1995). Reliable values of transition probabilities are needed for interpreting blends in observed spectra, for abundance studies and for modeling stellar atmospheres.

A powerful method for obtaining absolute transition probabilities is to combine measurements of normalized relative line intensities from a given energy level (branching fractions) with an absolute measurement of the level lifetime (Huber & Sandeman 1986). This procedure does not depend on any form of equilibrium in the population distribution over different levels, but it is essential that all significant lines from the level be included in the sum, and these may vary widely in wavelength.

Several groups have applied this method to different sets of Ti II lines. In 1990 Savanov, Huovelin, & Tuominem published a catalog of oscillator strengths incorporating weighted measurements from 10 sources, with lifetimes rescaled where relevant to the beam foil measurements of Roberts, Anderson, & Sorensen (1973). This catalog contains 419 lines from 244 to 542 nm and includes the results of Danzman & Kock (1980) by a combination of emission and hook methods for 67 lines in the range 305–542 nm. Ryabchikova (1994) renormalized existing data for the visible region to absolute astrophysical values and obtained good agreement with Danzman & Kock; they estimated their uncertainties to be about 0.08 dex for relative and 0.15 dex for absolute *f*-values.

The incentive for the present work was a new set of radiative lifetimes for 42 levels of Ti II measured by Bizzarri et al. (1993) by time-resolved laser fluorescence on slow ionic beams. Transition probabilities for 100 lines between 305 and 993 nm originating from seven of these levels were found from branching fractions measured by high-resolution Fourier transform spectroscopy (FTS) at the US National Solar Observatory. The wide spectral range and good resolution and luminosity of FTS make it a particularly suitable technique for measuring branching fractions. Bizzarri et al. did not report branching fractions for the lines originating from the other 35 levels for which they had measured lifetimes because they were primarily interested in weak lines suitable for determining the solar abundance of titanium. In any case the number of complete sets of branching fractions they could obtain was limited by the short-wavelength cutoff of their FT spectrometer.

The extensive calculations of Kurucz (2000) on energy levels and *gf*-values for astrophysically important atoms and ions include, of course, Ti II. His *gf*-values for strong lines are well known to agree rather well with experimental values, but for weak lines they are inevitably more uncertain. In the case of Ti II, Grevesse & Noels (1993) have compared the solar abundance derived from the *gf*-values measured by Bizzarri et al. (1993) with that derived from the same lines using Kurucz's calculated *gf*-values: the latter has a lower mean and a much greater scatter (0.3 dex as against 0.04 dex). Normalization of Kurucz's data to measured lifetimes makes little difference because the calculated lifetimes are determined predominantly by the transition probabilities of the strong lines.

We have used the UV FT spectrometer at Imperial College with a Ti hollow cathode lamp to extend branching fraction measurements to shorter wavelengths, covering more than 600 Ti II lines from 83 levels. The levels range in energy from 29,544 to 69,084 cm^{-1}, and our spectra extend from 16,600 to 53,000 cm^{-1} (602–187 nm), overlapping those of Bizzarri et al. in the region from 602 to 305 nm. The measured lifetimes of these authors have been used to convert the branching fractions to absolute *gf*-values for 39 of these levels. For the remaining 44 we have used Kurucz's calculated lifetimes. For a further six levels that are less than 95% complete we report branching ratios for the remaining lines.

2. EXPERIMENTAL PROCEDURE

There are three steps in the experimental determination of oscillator strengths by the branching fraction method. The first is to record each spectrum together with an appropriate calibration spectrum from an intensity standard, resulting in an intensity-calibrated line list (on a relative

scale) for that spectrum. Several such spectra are required, both because of the wide spectral range (requiring two different calibration lamps) and because of the need for different lamp currents, as explained below. The second step is to collect all lines from a given upper level and put them on the same relative intensity scale, using lines that are common to two spectra to provide the scaling factor. The final stage is to derive branching fractions from the relative intensities by normalizing each set from a given upper level to unit sum, making allowance where necessary for any lines missing from the set; the lifetime of the upper level, measured or calculated, is then used to convert the branching fractions to absolute transition probabilities or *f*-values.

2.1. *Measurements*

The light source was a Ti hollow cathode lamp with argon at 2 mbar pressure as carrier gas. The hollow cathode itself was an open-ended cylinder of pure titanium 20 mm long with an internal diameter of 8 mm. The body of the lamp was water-cooled and acted as the anode. Currents ranged from 25 mA to 500 mA, the lower currents being necessary to avoid self-absorption in some of the stronger lines (see below).

The Fourier transform spectrometer was a Chelsea Instruments FT500, based on the laboratory prototype designed and built at Imperial College (Thorne et al. 1987), with a short-wavelength limit of about 178 nm. The spectral range to be covered was divided into three overlapping regions, approximately 601–370, 420–250, and 290–187 nm. The first of these was defined by a 1P28 photomultiplier tube with a short-wavelength cutoff filter in the form of a piece of crown glass, the second by a 1P28 photomultiplier tube with a UG5 filter, and the third by a solar-blind photomultiplier tube (Hamamatsu R166) with a short-wavelength cutoff set by oxygen absorption in the path outside the interferometer. A typical two-sided interferogram had about one million samples, giving half a million spectral points. The Doppler widths of the hollow cathode lines ranged from about 0.12 cm^{-1} at 600 nm to 0.36 cm^{-1} at 190 nm, and the spectra were taken with resolutions of 0.04, 0.045, and 0.05 cm^{-1} respectively, to give at least 3 points per line width. Scan times were typically 6 minutes, but several interferograms were co-added; the total time to take one spectrum was 1 to 2 hours, including the intensity calibrations. The signal-to-noise ratio improved, as expected, with the square root of the number of co-added interferograms, but 2 hours represented a practical limit because of the drifts in alignment of the interferometer. Between each series of runs the lamp window was cleaned with nitric acid to avoid errors in intensity calibration arising from sputtered metal on the window.

The Ti line lists were compiled from the phase-corrected spectra and processed with the GREMLIN set of programs developed by J. W. Brault (2000, private communication). A least squares fit to a Voigt profile for each line was performed, and the relative intensity of the line in wavenumber units was represented by the integral over this profile (the equivalent width).

Inspection of the preliminary Ti data revealed that self-absorption was a problem with some of the strong lines when the lamp was run at 500 mA to bring up the weak lines. The flattening of the line peak of a fully resolved line due to self-absorption results in a characteristic signature in the residuals of the fit to a Voigt profile that is easily recognized (see Fig. 1). The experiments were therefore repeated at lower currents down to 25 mA. It was found that 200 mA was sufficiently low to produce negligible self-absorption for strong lines in the visible region, whereas it was necessary to go down to 50 mA, or, in a few cases, to 25 mA for the stronger lines in the UV.

2.2. *Intensity Calibration*

We describe the intensity calibration procedure in some detail because it is a potential source of systematic errors.

In FTS the instrument response depends not only on the detector characteristics and the transmissivity and reflectivity of the optical components but also on the modulation achieved in the interferogram. This is set by the errors in the recombining wavefronts, and it is always wavelength depen-

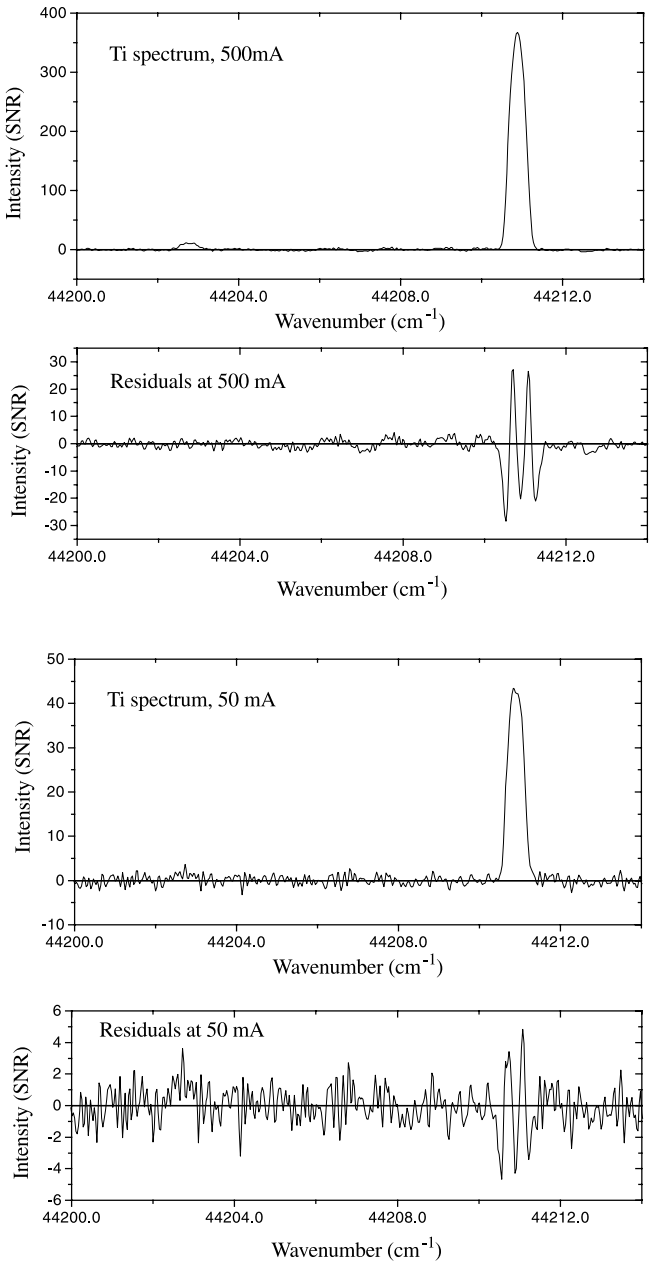

FIG. 1.—Two lines in the spectrum of Ti II recorded at 500 mA and 50 mA together with the residuals remaining after fitting the lines with a least squares fit to a Voigt profile. The weaker line has not been fitted in the 50 mA run. All plots are normalized to set the rms noise equal to unity.

dent. Two dangers must be guarded against. The modulation normally decreases slowly with time, falling off more rapidly at shorter wavelengths, and it depends on the area of the beamsplitter that is illuminated. Both of these difficulties can be overcome by calibrating from the relative intensities of Ar lines generated in the hollow cathode itself (Bizzarri et al. 1993; O'Brian et al. 1991). Previous experiments used branching ratios from several sets of Ar I and Ar II lines measured by Adams & Whaling (1981), which have a short-wavelength limit of 290 nm. Subsequently, Hashiguchi & Hasikuni (1985) measured branching ratios for Ar II lines from 500 to 200 nm. A later compilation of Ar I and Ar II branching ratios for spectrometer response calibration by Whaling, Carle, & Pitt (1993) covers the wavelength range 459–210 nm and includes new measurements by the authors, but all the branches below 290 nm are taken from Hashiguchi & Hasikuni. More recently Siems et al. (1996) measured branching ratios for Ar II lines from 9 upper levels over the range 230–160 nm, obtaining good agreement with Hashiguchi & Hasikuni over the rather limited overlap region. Unfortunately, it was not possible to use these Ar II branching ratios to calibrate the titanium spectra because at short wavelengths only the stronger Ar lines appeared at sufficiently good signal-to-noise ratio to be useful. There are two reasons for this: the measurements of branching ratios were made with hollow cathodes of either graphite (Hashiguchi & Hasikuni 1985) or aluminum (Siems et al. 1996), both of which sputter relatively badly so that the signal-to-noise ratio is not degraded by lines from the cathode material, and the currents used were either comparable with our high-current runs (Hashiguchi & Hasikuni 1985) or as high as 3 A (Siems et al. 1996). The spectral coverage provided by the few good lines in our low-current runs was inadequate for intensity calibration.

We therefore used a calibrated tungsten halogen lamp (100 W) for the visible and near-UV regions ($\lambda > 300$ nm) and a calibrated deuterium lamp (Cathodeon VO4, 300 mA) for the UV ($\lambda < 400$ nm) to determine the instrument response directly. These lamps were calibrated respectively for relative spectral radiance and relative spectral irradiance at the National Physical Laboratory (NPL). The calibration lamp and the Ti lamp were mounted at similar distances from the entrance aperture of the FT spectrometer, with a mirror to switch between them. A lens formed an enlarged image of both sources sufficiently close to the entrance aperture to ensure that they both used the full beamsplitter area. The modulation drift was allowed for by taking calibration spectra both before and after each Ti spectrum, discarding any runs in which the two calibration spectra showed significant differences.

It should be noted that the calibration data are provided in the form of relative spectral radiance or irradiance per unit wavelength interval. The response of an FT spectrometer used with a photon detector is proportional to photon flux per unit wavenumber interval, so energy per wavelength interval must be converted to photons per wavenumber interval before applying the calibration. As the energy-to-photons conversion scales with λ and the $\Delta\lambda$ to $\Delta\sigma$ conversion scales with λ^{-2}, the NPL data have to be scaled by λ^3 to find the correct instrument response. Because of the line structure in the deuterium spectrum it is important that the calibration spectrum should have the same spectral resolution as the instrument used by NPL to calibrate the lamp, which was a grating spectrometer with a slit width corresponding to 2 nm. We therefore interpolated our lamp spectrum onto a linear wavelength scale and convolved it with a function equivalent to a 2 nm slit before dividing by the scaled NPL values to obtain a set of numbers corresponding to the FT spectrometer response. These numbers were interpolated back onto a wavenumber scale to give the response curve used for the Ti intensity calibration. This procedure again used the GREMLIN set of programs (J. W. Brault 2000, private communication). Figure 2 shows typical response curves for the three spectral regions.

2.3. *Combining of Spectra*

The output from the first stage was six spectra, one at high and one at low current from each of three spectral regions, each calibrated on its own relative intensity scale. The second step was to collect the set of all lines from each upper level from the six spectra and put them on a common intensity scale. We used the calculations of Kurucz (2000) to define the line list for each set, with an intensity cutoff of log $gf > -3.0$. In the fairly frequent cases where no line showed evidence of significant self-absorption, the low-current spectra could be discarded. Otherwise the strongest lines of the set that were free of self-absorption in the high-current run were used to scale the corresponding low-current run. The scaling factors were usually averaged over all the levels in the relevant multiplet to reduce the random errors, on the grounds that the relative excitation is likely to be constant for levels only a few hundred cm^{-1} apart.

Lines from the same upper level in different spectral regions (but taken at the same lamp current) were related by using lines in the overlap region to provide the scaling factor. Ideally, these transfer lines also should have the same upper level, or at least a level in the same multiplet, as the two sets of lines they are connecting. Because of the way the lines are grouped, and the rather small overlap (≈ 4000 cm^{-1}) between the visible and the near-UV spectra, this was not always possible. However, for two spectra taken with very similar lamp running conditions, the scaling factor might be expected to be the same for all lines. For the 15 lines that were reasonably strong in both spectra, the scaling factor was in fact constant to $\pm 6\%$ (standard deviation), independent of the upper energy level, and this uncertainty is incorporated in the final errors. The

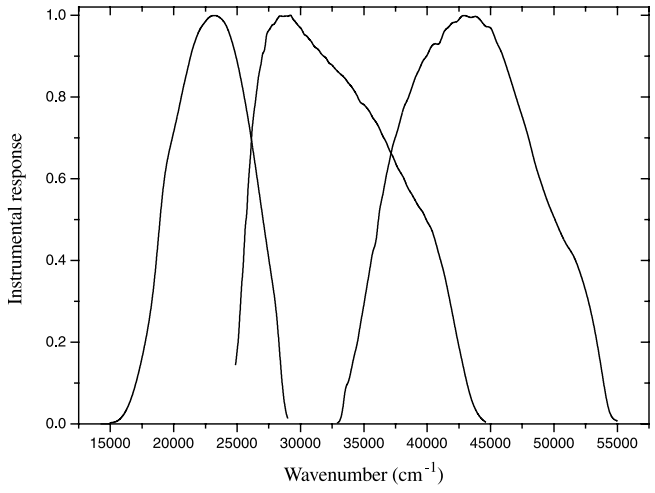

FIG. 2.—Instrumental response curves for the three spectral ranges observed in this work.

fact that the scaling factor also shows no significant wavelength dependence also shows that the calibrations from the tungsten and deuterium lamps agree to within their stated uncertainties (2% and 5% respectively—see § 3) over this very limited wavenumber range. (A direct comparison of the instrument response curves found using the two lamps was not possible because the spectra were taken with different filters).

2.4. *Derivation of Branching Fractions and Absolute gf-Values*

After intensity calibration the integrated area of each line is proportional to its intensity Φ_{ij} in photons per second. Its branching fraction F_{ij} is then given by

$$F_{ij} = \frac{\Phi_{ij}}{\Sigma_j \Phi_{ij}}, \quad (1)$$

where the sum is taken over all lines from a given upper level i. The calculations of Kurucz (2000) were used not only to define the complete set of lines but also to estimate the contribution from missing lines. Lines may be missing because they are outside the spectral region of observation or because they are blended with another line (Ti I or Ar) or doubly identified. For most levels the missing fraction α is less than 5%, which is smaller than the uncertainty in the sum of the observed lines. In such cases we applied a correction factor $(1 + \alpha)$ to the sum in equation (1) to give the best estimate of the true value of each F_{ij}.

Absolute transition probabilities were obtained from the branching fractions in the usual way:

$$A_{ij} = \frac{F_{ij}}{\tau_i}, \quad (2)$$

where τ_i is the lifetime of the upper level, either measured or calculated (see § 3).

Lines that have predicted values of log gf greater than -3.0 but are below the noise level in our spectra can also be regarded as "missing" but can be assigned an experimental maximum gf-value. The noise level in FTS is independent of wavelength, and as there are about 3 spectral resolution elements per line width the detection limit corresponds to a peak value of about 2.5 times the rms noise. This limit can be converted to an integrated line intensity by comparison with neighboring lines, allowing an upper limit for branching fraction and log gf to be derived. Except for a few cases at the shortest wavelengths, where the detection limit is relatively high, the upper limits for these weak lines are within the errors of the sum in equation (1).

3. RESULTS AND DISCUSSION

The results are presented in Tables 1 and 2 for upper levels that have sufficiently complete sets of lines (>95%) to allow the derivation of reliable branching fractions. Those in Table 1 have been converted to absolute gf-values by means of the measured lifetimes of Bizzarri et al. (1993), and for those in Table 2, all lying above 50,000 cm^{-1}, we have used the calculated lifetimes of Kurucz (2000). Table 3 contains a few levels for which a significant line is inaccessible for various reasons; for these levels we have given branching ratios, corresponding to relative gf-values, for the remaining lines.

All three tables are arranged in order of increasing upper energy level, designated by its energy in cm^{-1} and its term assignment. In Table 1 the measured lifetime and associated uncertainty of Bizzarri et al. is given, followed by the percentage completeness of the set of transitions. For each line in the set we give the wavenumber, the air wavelength (or

TABLE 1

EXPERIMENTAL BRANCHING FRACTIONS FOR Ti II TRANSITIONS COMBINED WITH EXPERIMENTAL LIFETIMES TO GIVE ABSOLUTE TRANSITION PROBABILITIES AND log gf-VALUES

WN (cm^{-1})	Air Wl (nm)	Note	BF	Err_{BF}	A (s^{-1})	(±%)	log gf	(±dex)	log gf Kurucz	log gf Bizzarri	(±dex) Bizzarri
Level 29544 cm^{-1} $3d^2(^3F)4p\ z^4G_{2.5}$ 5.70 ns ± 5% 100% Complete											
20546.662.....	486.56114		0.04	0.01	7.65E+4	21.9	−2.79	0.09	−2.64	−2.81	0.04
20833.885.....	479.85315		0.06	0.01	1.01E+5	20.6	−2.68	0.08	−2.64	−2.67	0.05
24915.798.....	401.23835		0.57	0.05	9.97E+5	10.2	−1.84	0.04	−1.73	−1.75	0.03
28560.538.....	350.03331		0.41	0.02	7.24E+5	7.2	−2.10	0.03	−2.13	−2.02	0.03
28636.486.....	349.10494		3.66	0.16	6.41E+6	7.0	−1.15	0.03	−1.13	−1.06	0.03
29318.750.....	340.98083		0.57	0.03	9.96E+5	7.1	−1.98	0.03	−1.89	−1.89	0.03
29450.341.....	339.45720		15.33	0.87	2.69E+7	7.8	−.55	0.03	−0.52	−0.54	0.02
29544.451.....	338.37587		79.37	4.52	1.39E+8	7.7	0.16	0.03	0.20	0.15	0.02
24646.745.....	405.61852	u	0.07		1.20E+5		−2.75		−3.27		
Level 29734 cm^{-1} $3d^2(^3F)4p\ z^4G_{3.5}$ 5.6 ns ± 5% 100% Complete											
20990.281.....	476.27777		0.04	0.01	6.66E+4	30.6	−2.74	0.12	−2.89		
24836.902.....	402.51294		0.21	0.04	3.72E+5	18.4	−2.14	0.07	−2.09		
28647.264.....	348.97360		0.40	0.02	7.18E+5	7.0	−1.98	0.03	−2.09		

NOTES.—Table 1 is published in its entirety as a machine-readable table in the electronic edition of *The Astrophysical Journal*. A portion is shown here for guidance regarding its form and content. Columns are as follows WN, Vacuum wavenumber (wavenumbers from Zapadlik et al. except when transitions not observed by Zapadlik et al.); λ_{air}, wavelength in air for $\lambda > 200.0$ nm; BF, branching fraction, error in BF; A, absolute transition probability (s^{-1}); % error in A; log gf found by combining A and experimental lifetime; error (dex) in log gf, log gf Kurucz, calculated (R. L. Kurucz 1999, private communication), log gf and its error from Bizzarri et al. (1993). Annotations to transitions indicate: x, transition not observed in this work or in that of Zapadlik et al.; o, outside the observed spectral range of this work; b, blended line; d, a doubly identified line; i, observed in this work but not in that of Zapadlik et al. and hence wavenumbers and wavelengths are from this work; u, observed by Zapadlik et al. but not observed in this work. For lines annotated with x or u, the maximum possible branching fraction has been estimated and hence the maximum value of A and maximum possible log gf for that transition. No error in log gf is given for these transitions annotated x or u since it is an approximate estimate.

TABLE 2

EXPERIMENTAL BRANCHING FRACTIONS FOR Ti II TRANSITIONS COMBINED WITH CALCULATED LIFETIMES TO GIVE ABSOLUTE TRANSITION PROBABILITIES AND log *gf*-VALUES

WN (cm^{-1})	Air Wl (nm)	Note	BF	Err_{BF}	$A(s^{-1})$	(±%)	log *gf*	(±dex)	log *gf* Kurucz
Level 52330 cm^{-1}, $3d(^2D)4s4p(^3P)\ ^4F_{1.5}$, 7.0 ns, 100% Complete									
43619.340.....	229.18545		2.58	1.05	3.69E+6	40.6	−1.93	0.19	−2.18
52235.773.....	191.43969		6.28	1.63	8.96E+6	25.9	−1.71	0.14	−2.00
52329.889.....	191.09538		91.10	8.38	1.30E+8	9.2	−.55	0.08	−0.54
39701.61	251.8032	x	2.77		3.96E+6		−1.82		−2.58
42399.125.....	235.78180	u	2.58		3.69E+6		−1.91		−2.70
42456.988.....	235.46044	u	2.58		3.69E+6		−1.91		−2.84
47701.76	209.5693	x	4.58		6.54E+6		−1.76		−2.88
Level 52339 cm^{-1}, $3d(^2D)4s4p(^3P)\ ^4D_{0.5}$, 2.4 ns, 100% Complete									
42466.340.....	235.40858		14.60	2.54	6.07E+7	17.4	−1.00	0.11	−1.23
52339.243.....	191.06123		85.40	9.74	3.56E+8	11.4	−.41	0.09	−0.39
42408.66	235.7288	x	3.67		1.53E+7		−1.59		−1.97
42488.45	235.2861	x	3.67		1.53E+7		−1.60		−2.49

NOTES.—Table 2 is published in its entirety as a machine-readable table in the electronic edition of *The Astrophysical Journal*. A portion is shown here for guidance regarding its form and content. Columns are as follows: WN, Vacuum wavenumber (wavenumbers from Zapadlik et al. except when transitions not seen by Zapadlik et al.); λ_{air}, wavelength in air; BF, branching fraction, error in BF; *A*, absolute transition probability (s^{-1}); % error in *A*; log *gf* found by combining *A* and calculated lifetime; error (dex) in log *gf*—here the error in the calculated lifetimes (Kurucz) is included and estimated as 0.04 dex. Annotations to transitions indicate: x, transition not observed in this work or in that of Zapadlik et al.; o, outside the observed spectral range of this work; b, blended line; i, observed in this work but not in that of Zapadlik et al.and hence wavenumbers and wavelengths are from this work; u, observed by Zapadlik et al. but not observed in this work; d, a doubly identified line. For lines annotated with x or u, the maximum possible branching fraction has been estimated and hence the maximum value of *A* and maximum possible log *gf* for that transition. No error in log *gf* is given for these transitions annotated x or u since it is an approximate estimate.

vacuum wavelength if below 200 nm), the branching fraction, with error, the transition probability, with error, and the log *gf*-value, with error in dex. Kurucz's calculated log *gf*, and, where applicable, the measured log *gf* of Bizzarri et al. with experimental error (dex) are given for comparison. "Missing" lines are listed below the measured lines for each level, also with Kurucz's calculated log *gf*. For all such lines that are within our spectral region but below the detection

TABLE 3

EXPERIMENTAL BRANCHING FRACTIONS FOR INCOMPLETE SETS OF Ti II TRANSITIONS COMBINED WITH CALCULATED VALUES FOR MISSING LINES TO GIVE APPROXIMATE ABSOLUTE TRANSITION PROBABILITIES AND log *gf*-VALUES

WN (cm^{-1})	Air Wl (nm)	Note	BF	Err_{BF}	*A* (s^{-1})	(±%)	log *gf*	(±dex)	log *gf* Kurucz	log *gf* Bizzarri	(±dex) Bizzarri
Level 31490 cm^{-1}, $3d^2(^3F)4p\ z^2F_{3.5}$, 6.8 ns ± 4.4% (Bizzarri), 89.5% Complete, 0.07% Outside, 10.4% Blended											
18732.659.....	533.67859		0.51	0.02	7.46E+5	6.2	−1.59	0.03	−1.59	−1.63	0.03
21466.117.....	465.72004		0.15	0.01	2.21E+5	8.0	−2.24	0.03	−2.20	−2.32	0.03
21972.767.....	454.98126		0.12	0.01	1.82E+5	10.9	−2.35	0.05	−2.35	−2.33	0.05
22493.128.....	444.45545		0.16	0.01	2.40E+5	7.8	−2.24	0.03	−2.14	−2.21	0.03
22746.577.....	439.50311		8.46	0.13	1.24E+7	4.7	−.54	0.02	−0.45	−0.51	0.02
26593.200.....	375.92914		76.28	1.51	1.12E+8	4.8	0.28	0.02	0.31	0.27	0.02
30275.084.....	330.20953		0.23	0.02	3.37E+5	8.6	−2.36	0.04	−2.13	−2.33	0.03
30403.562.....	328.81410		0.49	0.03	7.25E+5	7.1	−2.03	0.03	−2.25	−1.97	0.03
30507.001.....	327.69917		0.15	0.01	2.28E+5	9.9	−2.53	0.04	−2.68	−2.48	0.07
31097.471.....	321.47669	d	2.19	0.11	3.22E+6	6.8	−1.40	0.03	−1.35	−1.34	0.03
31265.214.....	319.75185		0.60	0.03	8.78E+5	7.0	−1.97	0.03	−2.55	−1.90	0.03
31396.802.....	318.41169		0.18	0.02	2.71E+5	9.8	−2.48	0.04	−2.18	−2.47	0.04
6298.03	1587.3644	o	0.03						−1.92		
10599.16	943.2122	o	0.04						−2.12		

NOTES.—Table 3 is published in its entirety as a machine-readable table in the electronic edition of *The Astrophysical Journal*. A portion is shown here for guidance regarding its form and content. Table 3 presents branching fractions, absolute transition probabilities and log *gf*s for levels which have incompletely observed transitions. Columns are as follows: WN, Vacuum wavenumber (wavenumbers from Zapadlik et al. except when transitions not seen by Zapadlik et al.); λ_{air}, wavelength in air; BF, branching fraction, error in BF; *A*, absolute transition probability (s^{-1}); % error in *A*; log *gf* found by combining *A* and calculated or experimental lifetime; error (dex) in log *gf*—here, if the lifetime is calculated (Kurucz) then an estimated error in calculated lifetime of 0.04 dex is included. Annotations to transitions indicate: x, transition not observed in this work or in that of Zapadlik et al.; o, outside the observed spectral range of this work; b, blended line; i, observed in this work but not in that of Zapadlik et al. and hence wavenumbers and wavelengths are from this work; u, observed by Zapadlik et al. but not observed in this work; d, a doubly identified line. For lines annotated with x or u, the maximum possible branching fraction has been estimated and hence the maximum value of *A* and maximum possible log *gf* for that transition. No error in log *gf* is given for these transitions annotated x or u since it is an approximate estimate.

limit we give maximum values of branching fraction, transition probability, and log *gf*. Table 2 is identical to Table 1 except that the lifetimes are Kurucz's calculated values. As the uncertainties in the calculated lifetimes are unknown, we have arbitrarily assigned them a value of 10%, or 0.04 dex, based on the mean difference of 0.5 ns between the Kurucz and Bizzarri et al. values for the 42 levels measured by the latter. In Table 3 the branching ratios have been approximately normalized to a sum of unity by using Kurucz's calculated branching fraction for the missing line(s), but they must still be regarded as branching *ratios*, not branching *fractions*, and the quoted errors refer to their relative values only.

Tables 1, 2, and 3 contain all but four of the levels from 29,544 to 69,084 cm^{-1}. One of the four missing levels has only one transition, and the other three have significant transitions that are below our effective limit of 187 nm or are partly absorbed by lines from the O_2 Schumann-Runge bands (although the interferometer was evacuated, there was a long air path between the source and the interferometer).

Some comment is needed on the wavenumbers in these tables. The wavenumber scale in FTS is strictly linear, and in principle only one reference wavenumber is required to put it on an absolute scale. In practice several reference lines are used, but they do not need to be distributed through the spectrum as in grating spectrometry. At IC we have consistently calibrated our spectra from a set of 26 blue Ar II lines (Learner & Thorne 1988), originally measured against the ^{86}Kr standard by Norlén (1973). The calibration uncertainty is estimated to be within 0.001 cm^{-1} at 400 nm rising to 0.002 cm^{-1} at 200 nm. The precision with which the wavenumber of an individual line can be measured depends on its signal-to-noise ratio, varying from less than 0.001 cm^{-1} for a strong isolated line to, typically, 0.02 cm^{-1} for a weak line close to the detection limit. The FTS wavenumbers are therefore an order of magnitude more accurate than those of Huldt et al. (1982) which form the basis of the energy level compilation of Sugar & Corliss (1985). In parallel with this work, Zapadlik, Johansson, & Litzén (2001) at the University of Lund (UL) have reanalyzed the Ti II spectrum using FTS spectra recorded with an instrument almost identical with ours over the region 454–187 nm together with FT spectra from the National Solar Observatory at longer wavelength. Their work has now been submitted for publication (Zapadlik et al. 2001), and they have kindly supplied us with their line list. Although the UL wavenumber calibration derives from the same set of Ar II standards as ours, their measurement uncertainties are somewhat smaller because they averaged over several spectra taken at higher current densities. The two sets of wavenumbers agree to within the measurement uncertainties, but it is clearly undesirable to have in the literature two sets of wavenumbers that are very similar but not identical. By agreement with UL, we have used their wavenumbers for all lines in Tables 1, 2, and 3 that appear in their list. Lines marked with an "i" do not appear in the UL list, and the wavenumbers given are our calibrated values; all such lines are weak, with uncertainties from 0.01 to 0.03 cm^{-1}. Lines that are absent from both the UL and IC lists are marked with an "x" and identified by the wavenumbers in Kurucz's calculations; they have been rounded to seven significant figures to reflect the lower accuracy. Lines outside the spectral region of observation (marked "o") and blended lines (marked "b") have been similarly rounded.

The errors in relative intensity for each measured line in the tables incorporate the uncertainties in the individual line intensity measurements and in the calibration of the standard lamp. The first of these is set by the signal-to-noise ratio of the line itself together with the errors in the transfer ratios needed to put lines from different spectra onto a common scale as described in § 2. The tungsten lamp calibration uncertainty (one standard deviation) is quoted by NPL as 1.25% and 2.0% respectively above and below 400 nm. For the deuterium lamp it is 5.0% and 4.0% respectively above and below 360 nm. As we are concerned only with relative intensities, we have ascribed $1/\sqrt{2}$ of the relevant calibration uncertainty to each line.

The uncertainty in the absolute transition probabilities and *gf*-values for the transitions from any level must include the errors for the normalization constant $\Sigma_j \Phi_{ij}$ and the lifetime τ_i. The normalization error $d\Sigma$ is obtained by adding in quadrature the errors in relative intensity for all observed lines in the set, and it is dominated by the error in the strongest lines. The uncertainty in the unobserved fraction α can be ignored because, for the levels in Tables 1 and 2, α itself is comparable with or less than $d\Sigma/\Sigma$. In Table 1 we have included the errors in the lifetime measurements of Bizzarri et al. (1993), which are typically about 5%. In Table 2, as explained above, we have allowed 10% for the uncertainties in Kurucz's calculated lifetimes.

Figure 3 compares our log *gf*-values with those of Bizzarri et al. (1993) for the 55 lines common to both sets of measurements. Agreement is good for values of log *gf* down to −1.5, with a much wider scatter for the weaker lines. The plot is very similar to that shown by Bizzarri et al. comparing their results with the measurements of Danzman & Kock (1980). In Figure 4 our log *gf*-values are compared with the calculations of Kurucz for upper levels below 50,000 cm^{-1}. Although the distribution looks similar to that of Fig. 3, with a small spread for values down to −1.0, the scatter for the weaker lines is about an order of magnitude greater (standard deviation 0.28 dex, or nearly a factor of 2, as against 0.07 dex, or 17%). Renormalizing the calculated *gf*-values to the measured lifetimes would simply shift the data points down by 0.04 dex on average, making very

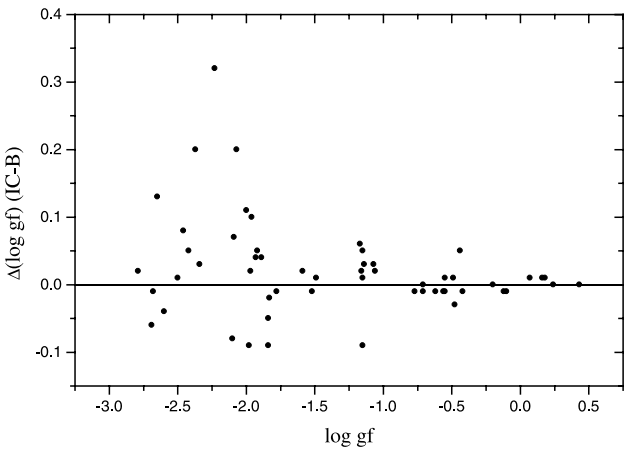

FIG. 3.—Comparison of the values of log *gf* determined in this work with those determined by Bizzarri et al (1993).

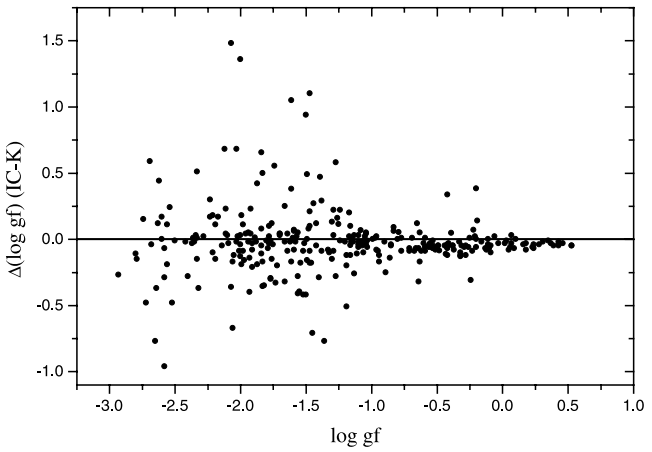

FIG. 4.—Comparison of the values of log *gf* determined in this work with those calculated by R. L. Kurucz (2000) for the levels given in Table 1.

little difference to the plot. The comparison between our values and Kurucz's calculated values for the levels above 50,000 cm^{-1}, which are normalized to Kurucz's lifetimes, shows a very similar pattern, bearing in mind that in this case the strong lines are constrained to agree closely by the normalization.

Recently a new set of transition probabilities for 4*s*–4*p* transitions between the ground state term and six upper terms (44 lines in all) were calculated by Luke (1999) with configuration interaction involving up to 52 configurations.

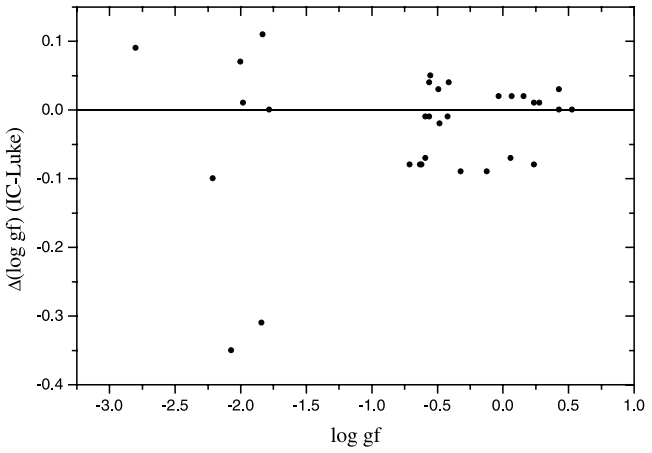

FIG. 5.—Comparison of the values of log *gf* determined in this work with those calculated by Luke (1999).

19 of these lines have transition probabilities measured by Bizzarri et al. Luke points out that for two of the upper terms his values are a little lower than those of Kurucz, agreeing more closely with the measured values of Bizzarri et al., but for the other two sets of "allowed" transitions ($\Delta S = 0$) the computed values agree with each other but not with the observations. For the weaker, "forbidden," transitions the computed rates agree much less well with each other or with the six measured values. Figure 5 compares our measured log *gf*-values from Table 1 with Luke's computed values (length formulation) for 32 lines from 15 of the 18 upper levels in his work (the other three levels are incomplete in our measurements). The plot confirms that the strong lines appear to fall into two groups, but the weak lines are too few in number to justify any useful conclusion.

4. CONCLUSION

The wide spectral range, high resolution, and linear response of FTS in the visible and UV spectral regions have been exploited to measure branching fractions in the astrophysically important ion Ti II for all but six of the 93 energy levels between 29,544 and 69,084 cm^{-1}. The branching fractions have been converted to absolute *gf*-values for 624 lines by means of the measured lifetimes of Bizzarri et al. (1993) for the 39 levels below 50,000 cm^{-1} and the calculated lifetimes of Kurucz (2000) for the remainder. Bizzarri et al. derived *gf*-values for 100 lines from their measured levels; we have increased this number to 317, with good agreement for the 55 lines in common. Comparison with the calculated *gf*-values of Kurucz for these 317 lines shows that nearly all strong lines ($\log gf > -1.0$) agree within the experimental uncertainties, but the scatter for the weak lines ($-3.0 < \log gf < -1.0$) is significantly greater than the experimental uncertainties. As lifetimes are determined primarily by the transition probabilities of the strong lines, the 307 absolute *gf*-values derived from the calculated lifetimes should also be reliable to within the experimental uncertainties.

This work forms part of our measurements on spectra of astrophysical importance, for which we acknowledge the support of the PPARC. The VUV FT spectrometer was developed with a grant from the Paul Instrument Fund of the Royal Society. J. C. P. is supported by a University Research Fellowship from the Royal Society. R. P. worked on this project with a Summer Studentship from IAESTE. We thank R. C. M. Learner and G. Cox for their valuable help.

REFERENCES

Adams, D. L., & Whaling, W. 1981, J. Opt. Soc. Am., 71, 1036
Bizzarri, A., Huber, M. C. E., Noels, A., Grevesse, N., Bergeson, S. D., Tsekeris, P., & Lawler, J. E. 1993, A&A, 273, 707
Danzman, K., & Kock, M. 1980, J. Phys. B, 13, 2051
Grevesse, N., & Noels, A. 1993, Phys. Scr., T47, 133
Hashiguchi, S., & Hasikuni, M. 1985, J. Phys. Soc. Japan, 54, 1290
Huber, M. C. E., & Sandeman, R. J. 1986, Rep. Prog. Phys., 49, 397
Huldt, S., Johansson, S., Litzen, U., & Wyart, J. -F. 1982, Phys. Scr., 25, 401
Johansson, S. 1995, in ASP Conf. Ser. 81, Laboratory and Astronomical High-Resolution Spectra, ed. A. J. Sauval, R. Blomme, & N. Grevesse (San Francisco: ASP), 151
Kurucz, R. L. 2000, http://cfaku5.harvard.edu/
Learner, R. C. M., & Thorne, A. P. 1988, J. Opt. Soc. Am., 2045 1988
Luke, T. M. 1999, Canadian J. Phys., 77, 571
Norlén, G. 1973, Phys. Scr., 8, 249
O'Brian, T. R., Wickliffe, M. E., Lawler, J. E., Whaling, W., & Brault, J. W. 1991, J. Opt. Soc. Am., B8, 1185
Roberts, J. R., Anderson, T., & Sorensen, G. 1973, ApJ, 181, 567
Ryabchikova, T. A., Hill, G. M., Landstreet, J. D., Piskunov, N., & Sigut, T. A. A. 1994, MNRAS, 267, 697
Savanov, I. S., Huovelin, J., & Tuominem, I. 1990, A&AS, 86, 531
Siems, A., Knauer, J. P., Kock, M., Johansson, S., & Litzén, U. 1996, J. Quant. Spectrosc. Radiat. Transfer, 56, 513
Sugar, J., & Corliss, C. 1985, J. Phys. Chem. Ref. Data, 14, Suppl. 2
Thorne, A. P., Harris, C. J., Wynne-Jones, I., Learner, R. C. M., & Cox, G. 1987, J. Phys. E, 20, 54
Whaling, W., Carle, M. T., & Pitt, M. L. 1993, J. Quant. Spectrosc. Radiat. Transfer, 50, 7
Zapadlik, I., Johansson, S., & Litzén, U. 2001, Phys. Scr., submitted